γ Irradiation of 2′-Deoxyadenosine in Oxygen-Free Aqueous Solutions: Identification and Conformational Features of Formamidopyrimidine Nucleoside Derivatives

Sébastien Raoul, Michel Bardet, and Jean Cadet*

CEA/Département de Recherche Fondamentale sur la Matière Condensée, SESAM/LAN, F-38054 Grenoble Cedex 9, France

Received February 21, 1995[⊗]

The two major radiation-induced decomposition products of 2′-deoxyadenosine in oxygen-free aqueous solution have been isolated by reverse-phase HPLC. The ^1H and ^{13}C NMR features of the two modified nucleosides obtained in DMSO-d_6 are indicative of a similar formamidopyrimidine structure for the base residue (the ring-opened form of a C-8 hydroxylated purine). Interestingly, the sugar moiety exhibits a pyranose configuration, the two nucleosides being a pair of α and β anomers. One-bond and long-range $^1H-^{13}C$ 2D NMR experiments have allowed the complete assignment of the carbon atoms. Confirmation of the base structure was obtained by $^1H-^{15}N$ scalar-correlated 2D NMR experiments. Attempts were made to characterize the expected furanose form of the initially generated formamidopyrimidine derivative. In this respect, isomerization reaction of the sugar moiety of the latter compound takes place rapidly after γ-irradiation as inferred from ^1H NMR analysis. The conformational study of the sugar moiety of the two pyranose anomers was inferred from detailed 600.13 MHz ^1H NMR analysis in D_2O. The α anomer exhibits a predominant $^1C_4$ conformation whereas the β anomer adopts preferentially a $^4C_1$ conformation. In addition, the dynamic study of the restricted rotation of the formamido bond has revealed a 1/5 ratio in favor of the *s-cis* rotamer for both nucleosides. The energy barrier at coalescence was determined to be $\Delta G^{\#} = 75.5$ kJ·mol^{-1} ($T_c = 370$ K).

Introduction

It is assumed that nucleic acids are the major cellular targets of the biological effects of ionizing radiation, including lethality, mutagenesis, and carcinogenesis (*1–4*). The major classes of radiation-induced DNA lesions include strand breaks and cross-links with proteins together with the modifications of the sugar and base moieties. The formation of the four main classes of DNA damage is, at least partly, rationalized in terms of the indirect action of radical species produced by the radiolysis of water. One of them, the hydroxyl radical (•OH), is the most reactive species toward both pyrimidine and purine bases. Whereas the structure assignment of the main radiation-induced decomposition products of pyrimidine bases has been widely established (*5–8*), the purines, especially adenine, have received much less attention (*9–11*). However, it was recently inferred from pulse radiolysis studies that •OH adds to C-4, C-5, and C-8 positions of the purines leading to the formation of both oxidizing and reducing radicals (*12*). In the latter case, it was shown that the main reducing radicals, namely, 8-hydroxy-7,8-dihydroadenyl (A8OH)[1] and 8-hydroxy-7,8-dihydroguanyl radicals, may undergo one-electron oxidation to give 8-hydroxypurines. A large number of studies report the identification and quantitation of the final stable products 8-oxo-7,8-dihydroadenine and 8-oxo-7,8-dihydroguanine and their nucleosides (for reviews see refs 5 and 13). However, in the total absence of oxidant (for example, in deaerated solution) A8OH may also undergo an unimolecular ring-opening transformation, followed by a reduction step to yield the formamidopyrimidine (FAPy) derivatives (*14*). The characterization of the FAPy derivatives upon exposure of 2′-deoxyguanosine to γ irradiation in deaerated solutions has been reported (*15*). In addition, exposure of adenine, as the free base, to ionizing radiation in deaerated aqueous solution was shown to give rise to 4,6-diamino-5-(formylamino)pyrimidine (FAPyAde) (*16*).

A few radiation-induced reactions of 2′-deoxyadenosine (dAdo) have been described. These included alteration and isomerization of the sugar moiety (*17*), the rupture of the N-glycosidic bond, and the C-5′–C-8 cyclization (*18*). In this study, we wish to report the isolation and the characterization of the two main stable final radiation-induced decomposition products of dAdo in deaerated aqueous solution: the α and β pyranose isomers of the FAPy derivatives (Chart 1). Extensive NMR spectroscopic measurements (including ^1H, ^{13}C and ^{15}N nuclei) were used to determine unambiguously the structure of the FAPy adducts. In addition, the study of the restricted rotation of the amide bond was performed by dynamic ^1H NMR spectroscopy, providing two distinct features for the *s-cis* and *s-trans* isomers; in this respect, spectral assignments were achieved. It should be added that the

* To whom correspondence should be addressed.

[⊗] Abstract published in *Advance ACS Abstracts*, July 1, 1995.

[1] Abbreviations: A8OH, 8-hydroxy-7,8-dihydroadenyl radical; dAdo, 2′-deoxyadenosine (**9**); FAPy, formamidopyrimidine; FAPyAde, 4,6-diamino-5-(formylamino)pyrimidine (**2**); β-f-FAPydAdo, 6-amino-4-[(2-deoxy-β-D-*erythro*-pentofuranosyl)amino]-5-(formylamino)pyrimidine (**4**); α-f-FAPydAdo, 6-amino-4-[(2-deoxy-α-D-*erythro*-pentofuranosyl)amino]-5-(formylamino)pyrimidine (**6**); β-p-FAPydAdo, 6-amino-4-[(2-deoxy-β-D-*erythro*-pentopyranosyl)amino]-5-(formylamino)pyrimidine (**3**); α-p-FAPydAdo, 6-amino-4-[(2-deoxy-α-D-*erythro*-pentopyranosyl)amino]-5-(formylamino)pyrimidine (**5**); TMS, tetramethylsilane; TSP, 3-(trimethylsilyl)propionate-*2,2,3,3-d*$_4$ sodium salt; RP-HPLC, reverse phase–high performance liquid chromatography; ODS, octadecylsilyl silica gel; HMQC, heteronuclear multi-quantum coherence; HMBC, heteronuclear multiple-bond correlation.

0893-228x/95/2708-0924$09.00/0

Chart 1

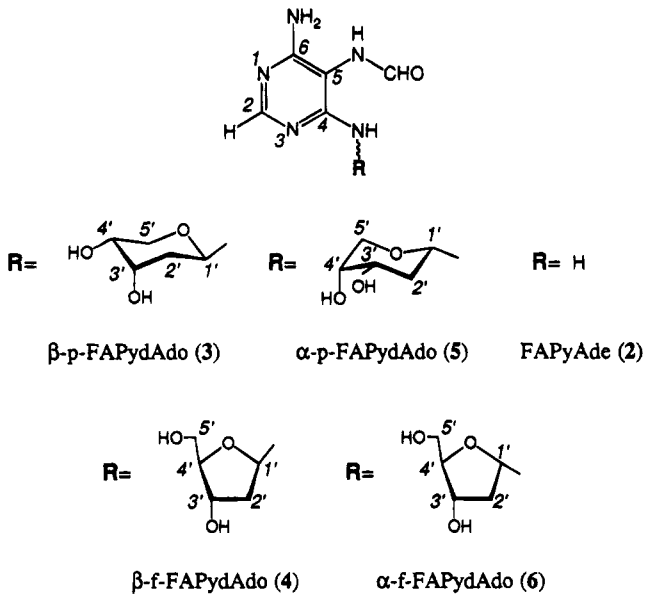

β-p-FAPydAdo (**3**) α-p-FAPydAdo (**5**) FAPyAde (**2**)

β-f-FAPydAdo (**4**) α-f-FAPydAdo (**6**)

s-cis/s-trans isomer ratio and the energy barrier to amide bond rotation were determined.

Experimental Procedures

Materials. dAdo (**9**) was purchased from Genofit SA (Geneva, Switzerland) and was used without further purification. FAPyAde (**2**) was obtained from Sigma Chemical Co. (St. Louis, MO). HPLC grade methanol was a Carlo Erba (Farmitalia Carlo Erba, Milan, Italy) product. Deuterium oxide (D_2O, 99.96% D) and deuteriated dimethyl sulfoxide (DMSO-d_6, 99.96% D) used for NMR spectroscopy were purchased from Eurisotop-CEA (Saclay, France). Water was purified with a Millipore-Milli-Q system.

γ Irradiation. γ radiolysis of deaerated aqueous solution of 2 mM dAdo (100 mg) was carried out with ^{60}Co sources located in a 5 m depth pool. The dose rate was determined to be 50 Gy/min according to the Red Perspex (Harwell, AEA Technology, Didcot, U.K.) dosimetry method. The solution was deaerated by bubbling nitrogen gas for 20 min prior to γ irradiation. The solvent was removed by rotary evaporation and the residue resuspended in a minimum volume of water prior to HPLC analysis.

High Performance Liquid Chromatography. The HPLC system consisted of two Model 302 HPLC pumps connected to a Model 811 dynamic mixer (Gilson, Middelton, WI), a Model LP-21 pulse damper (Scientific System Inc., State College, PA), a Sil-9A Shimatzu automatic injector (Touzard & Matignon, Paris, France), and a L-4000 UV variable wavelength spectrophotometer (Merck, Darmstadt, Germany). These instruments were connected to an Apple IIe computer which controls the mobile phase composition (after 5 min of 100% Milli-Q water, a linear gradient of methanol was introduced at a rate of 2%/min and a flow rate of 2 mL/min) and to a Data Master Model 621 (Gilson) which analyzes the signal coming from the UV detector. The semipreparative (250 × 6.2 mm i.d.) reverse phase column was home-packed with 10 μm Nucleosil octadecylsilyl silica gel (Nucleosil 100-10 C_{18}, Macherey-Nagel, Düren, Germany).

Spectroscopic Measurements. UV absorption spectra were obtained in water with a Hewlett-Packard 8452A diode array spectrophotometer (Amsterdam, The Netherlands). Fast atom bombardment (FAB) mass spectra were recorded in the positive mode with a ZAB 2-SEQ spectrometer (Fisons-VG, Manchester, U.K.) equipped with an LSIMS source. The molecules were dissolved in a glycerol–thioglycerol matrix containing 0.1 N NaI and then desorbed upon exposure to a 35 keV cesium ions beam. The ^1H NMR spectra were recorded in the Fourier transform mode by using AMX 600, AM 400, and AC 200 Brüker apparatus. Conformational studies were realized in D_2O, and spectral assignments of the proton signals were achieved by homonuclear decoupling experiments. To verify the assignments and to obtain accurate chemical shifts and coupling constants, the spectra were computer-simulated using the iterative LAOCOON III and PANIC Brüker programs. The chemical shifts were determined with respect either to 3-(trimethylsilyl)propionate-2,2,3,3-d_4 sodium salt (TSP) in D_2O or tetramethylsilane (TMS) in DMSO-d_6 as the internal references. The proton-coupled and -decoupled ^{13}C NMR spectra and two-dimensional $^1H-^{13}C$ and $^1H-^{15}N$ heteronuclear spectra were obtained with a Varian Unity 400 spectrometer. The latter experiments were carried out in DMSO-d_6. For the ^{13}C NMR experiments, the signal of the solvent was used as the secondary reference set at 39.5 ppm. *N,N*-Dimethylformamide was used as a secondary reference set at −275.2 ppm with respect to CH_3NO_2, for the ^{15}N NMR experiments. Thus, the ^{15}N chemical shifts are reported in ppm on the CH_3NO_2 scale (*19*). For one-bond and long-range $^1H-^AX$ (where $^AX = {}^{13}C$ or ^{15}N) scalar-correlated 2D NMR experiments (HMQC and HMBC, respectively), standard Varian software was used. This involved the utilization of standard pulse sequences provided by the constructor with the parameters indicated below. Theoretically, the optimum delay required to observe long-range correlations in the HMBC experiments is $1/[2 \times {}^nJ(X,H)]$, where $^nJ(X,H)$ is the long-range coupling constant. The $^2J(C,H)$ coupling in an aromatic system is usually small (2–3 Hz) whereas $^3J(C,H)$ coupling is within the range 7–15 Hz. Consequently, we used the values of 100, 80, and 60 ms for this delay. For ^{15}N, the delay was optimized for $^nJ(N,H) = 10$ Hz ($n = 2$ or 3). The delay for polarization transfer in HMQC experiments was set for $^1J(C,H) = 167$ Hz on one hand and for $^1J(N,H) = 90$ Hz on the other hand. Spectra were recorded at 293–301 K unless otherwise indicated, using an indirect 5 mm HX probe. The Brüker AM 400 spectrometer was used for the dynamic study involving heating of the sample within the temperature range 295–390 K with a 5 K increment. The error for the T_c determination was 5 K, and consequently, the error for the $\Delta G^{\#}_{370}$ value is estimated to be 1.1 kJ.mol^{-1}.

Results and Discussion

HPLC Separation of the Radiation-Induced Decomposition of 2′-Deoxyadenosine (9). An almost complete separation of the radiation-induced decomposition products of 2 mM dAdo (**9**) in deaerated aqueous solution was achieved on a semipreparative ODS column by using water as the mobile phase. A linear gradient of methanol was necessary to remove unmodified dAdo (**9**) which is known to be the more retained DNA nucleoside on reverse phase HPLC columns (*20*). A typical separation on a Nucleosil ODS column that was obtained after leaving the irradiated solution for 72 h at room temperature is reported in Figure 1. It should be noted that, under the conditions of γ radiolysis used (2.25 kGy), the degradation of dAdo (**9**) never exceeded 20%.

The three major HPLC eluting peaks with retention times of 7.0, 7.9, and 12.6 min were found to contain FAPyAde (**2**) and the β and α anomers of the pyranose forms of the FAPy derivatives **3** and **5**, respectively. It should be noted that **2** and **3** cannot be completely separated under the present analytical conditions. The latter compounds represent more than 50% of the overall radiation-induced decomposition products of dAdo under anoxic conditions. The two small HPLC peaks on each side of the α pyranose-containing fraction correspond to the unstable β and α furanose FAPy derivatives **4** and **6**, respectively. Due to the opening of the imidazole ring with concomitant appearance of hydrophilic groups (such as amine and formamide), the major radiation-induced

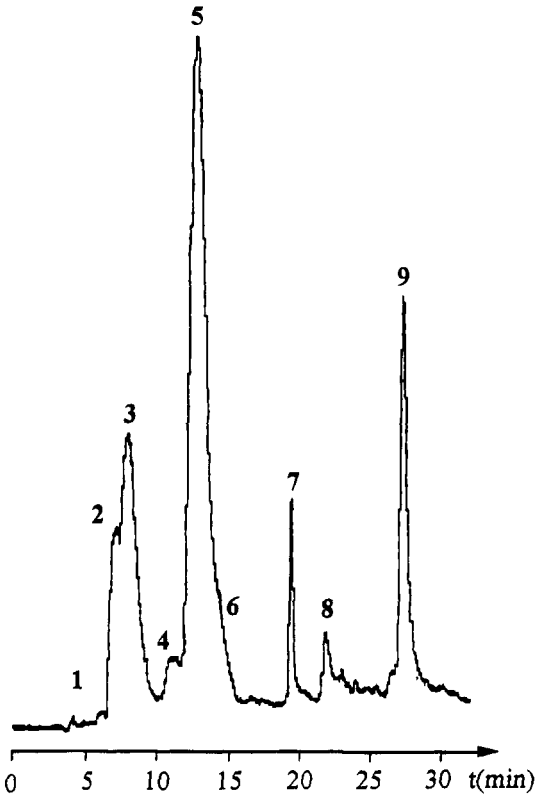

Figure 1. RP-HPLC profile of the radiation-induced degradation products of dAdo (**9**) in deaerated aqueous solution after leaving the solution 72 h at room temperature. UV detection at λ = 225 nm. The insoluble excess of dAdo after concentration by rotary evaporation was removed by centrifugation, and the supernatant only was injected onto the column.

degradation products **2**–**6** are eluted more rapidly on the ODS column than the parent dAdo (**9**).

Adenine (**8**) and dAdo (**9**) were identified by comparison of their retention times with those of commercially available authentic products analyzed under the same conditions. The product **7** with a retention time of 19 min was identified as the (5′*R*) diastereoisomer of 8,5′-cyclo-2′-deoxyadenosine (*18*). Analysis of the proton chemical shifts and coupling constants obtained in D_2O is indicative of a cyclic product: the loss of the H-8 and H-5″ signals together with the small coupling constants $J_{1'-2'}$, $J_{3'-4'}$, and $J_{4'-5'} \leq 1$ Hz are consistent with the already described product. The pyranose and furanose anomers of dAdo (**9**) were also shown to be produced under similar conditions of irradiation (*17*) but in very low yields. These compounds are expected to exhibit intermediate retention times between those of adenine (**8**) and dAdo (**9**). It may be added that the fraction **1** which elutes just after the void volume contains 2-deoxy-D-*erythro*-pentose.

Characterization of β-p-FAPydAdo (3) and α-p-FAPydAdo (5). The two main radiation-induced degradation products **3** and **5** appear to be two isomers according to their UV, FAB mass spectroscopy, and ^1H, ^{13}C, and ^{15}N NMR features. The UV spectra in water of both compounds (and this applied also to FAPyAde (**2**)) show the same absorbance properties with two maxima at 220 nm and a smaller one at 262 nm. The latter absorption peak is indicative of a partial loss of aromaticity compared to the parent dAdo (**9**). The positive FAB mass spectra of **3** and **5** exhibit a major pseudomolecular ion at m/z 270.0 ($[M + H]^+$) together with a characteristic fragment at m/z 154.1 ($[BH + H]^+$) which corresponds to the aglycon. This shows a gain of 18 amu in the base moiety as the result of addition of a molecule of H_2O to the starting dAdo (**9**). In addition, the presence of quasi-molecular ions at m/z 292.0 ($[M + Na]^+$) and m/z 362.1 ($[M + H + glycerol]^+$), respectively, provided further support to this hypothesis. The fragment at m/z 126.0 is indicative of the loss of carbon monoxide from the base, suggesting the presence of a carbonyl group within the aglycon of the molecules. Indirect confirmation of the occurrence of an isomeric relationship between **3** and **5** was provided by the comparison of the HPLC retention time, UV, and mass spectrometric features of the aglycon part obtained by mild acidic hydrolysis of the two nucleosides. They were found to be indistinguishable and identical to those of authentic FAPyAde (**2**). Additional relevant structural information was obtained by extensive ^1H, ^{13}C, and ^{15}N NMR spectroscopy analyses.

Table 1. ^1H NMR Chemical Shifts (ppm) of the Base Moiety of the FAPy Derivatives[a] (Major Rotamer)

δ (ppm)	NH-5	CHO	H-2	NH_2-6	NH-4
FAPyAde (**2**)	8.89	8.21	7.86	6.07	6.07[b]
β-p-FAPydAdo (**3**)	8.90	8.20	7.99	6.22	6.55
α-p-FAPydAdo (**5**)	8.95	8.24	7.99	6.22	7.00

[a] All spectra were obtained in DMSO-d_6 at 400.13 MHz. [b] Due to the symmetry of the molecule, the two NH_2 groups are equivalent and their signals appear as a singlet with an intensity of 4 protons.

Inspection of the ^1H NMR features of the FAPyAde (**2**) and isomers **3** and **5** obtained in DMSO-d_6 reveals the presence of a doublet (^3J(H,H) = 1.3 Hz) in the low field region (δ = 8.2 ppm) of the spectra (see Table 1). Two-dimensional ^1H–^1H COSY analysis of FAPyAde (**2**) shows a scalar correlation between the latter proton and the one resonating at 8.89 ppm. Furthermore, addition of D_2O leads to a collapse of the doublet (δ = 8.21 ppm) into a singlet due to the chemical exchange of a vicinal NH-type proton. The two involved protons were thus attributed to those belonging to a formamido group. Another doublet with a large coupling constant was found to resonate at δ = 6.55 and 7.00 ppm for the isomers **3** and **5**, respectively. The signal was assigned to those of the NH-4 by homonuclear decoupling of the anomeric proton H-1′. The vicinal $H_{1'}$–$C_{1'}$–N_4–H_4 couplings were measured in DMSO-d_6 (^3J(H,H) = 9.5 Hz for **3** and ^3J(H,H) = 9.2 Hz for **5**) but are not easily treated in terms of conformation around the $C_{1'}$–N_4 bond. The small observed differences (≤0.05 ppm) in the respective proton chemical shifts of the base moiety of **3** and **5**, with the exception of the NH-4, are consistent with a similar structure. One the other hand, the largest difference concerns the NH-4 resonance signals ($\Delta\delta$ = 0.45 ppm). This may be explained by the close proximity of the sugar moiety, which should affect the proton environment. The isomeric relationship within the sugar moiety of **3** and **5** was further confirmed by detailed ^1H NMR analysis in D_2O (*vide infra*).

The ^{13}C resonance signals of the sugar moiety of β-p-FAPydAdo (**3**) and α-p-FAPydAdo (**5**) were assigned by selective proton decoupling experiments and further confirmed by ^1H–^{13}C heteronuclear scalar-correlated 2D NMR experiments. The ^{13}C chemical shifts and ^1J(C,H) coupling constants of **2**, **3**, and **5** are reported in Table 2. The three molecules show similar values for the respective ^{13}C chemical shifts of the base. The C=O and C-2 (both attached to a proton) of the aglycon part of the nucleosides were easily assigned by examining ^1H–^{13}C scalar correlations. The doublet at 161 ppm was assigned

Table 2. ^{13}C NMR Chemical Shifts (ppm) and Coupling Constants (Hz) of the FAPy Derivatives[a] (Major Rotamer)

δ (ppm)	CHO	C-2	C-4	C-6	C-5	C-1′	C-2′	C-3′	C-4′	C-5′
FAPyAde (**2**)	160.7 (^1J = 196.4)[b]	155.6 (^1J = 193.6	159.4 (^3J = 11.3)[c]	159.4 (^3J = 11.3)	93.9					
β-p-FAPydAdo (**3**)	161.2 (^1J = 197.3)	155.7 (^1J = 194.8)	157.3 (^3J = 10.7	159.7 (^3J = 11.1)	94.8	74.0 (^1J = 151.7)	37.0 (^1J = 127.8)	67.0 (^1J = 141.3)	66.5 (^1J = 144.4)	64.4 (^1J = 144.0)
α-p-FAPydAdo (**5**)	161.1 (^1J = 195.3)	155.6 (^1J = 194.7)	157.1 (^3J = 10.7)	159.7 (^3J = 11.1)	94.6	75.5 (^1J = 156.9)	34.3 (^1J = 129.2)	67.7 (^1J = 141.4)	66.7 (^1J = 141.5)	63.9 (^1J = 143.3)
dAdo (**9**)	140.1[d]	152.8	149.2	156.4	119.6	84.5	40.0	71.4	88.3	62.3

[a] All spectra were obtained in DMSO-d_6 at 100.57 MHz. [b] ^1J refers to ^1J(C,H). [c] ^3J values are the coupling constants between the respective carbon atoms and H-2. [d] Chemical shift of the C-8.

to that of the carbon of the formamido group. The chemical shift of the C-2 is slightly downfield shifted by comparison with that of the parent compound dAdo ($\Delta\delta \approx 2.8$ ppm). The three quaternary carbons (C-4, C-5, C-6) were unambiguously attributed by heteronuclear $^1H-^{13}C$ multiple bond correlation NMR spectroscopy. The proton-coupled ^{13}C NMR spectra show ^3J(C,H) coupling constants between H-2 and C-4 (^3J(C,H) = 10.7 Hz) on one hand and C-6 on the other hand (^3J(C,H) = 11.1 Hz) (Table 2). These values are similar to ^3J(C,H) = 11.8 Hz and ^3J(C,H) = 11.5 Hz between H-2 and C-4 and C-6 observed in the case of 8-oxo-7,8-dihydroadenosine (*21*). For symmetrical reasons, C-4 and C-6 of the FAPyAde (**2**) have the same chemical shift, but the C-4 resonance signal of the nucleosides **3** and **5** is upfield shifted by about 2 ppm. The latter carbon atom was assigned to the 4-position taking into consideration the three- and two-bond correlations with the H-1′ and NH-4, respectively. The NH-4 proton of compound **5** also shows two three-bond $^1H-^{13}C$ correlations with the C-5 (δ = 94.6 ppm) and C-2′ (δ = 63.9 ppm) carbons, respectively. Assignment of C-6 was inferred from the observation of long-range correlations with NH-5 and H-2 protons, respectively.

The C-1′ carbon is the only carbon with two directly attached heteroatoms; thus, its resonance signal appears at lower field than the other remaining four carbons. In contrast, the dehydroxy-C-2′ signals of compounds **3** and **5**, attached to two carbons, were found to resonate at highest field. Although the C-5′ has a similar structure (*e.g.*, a methylene group), the α position of the oxygen atom is responsible for the observed 30 ppm downfield shift. The main striking difference in the ^{13}C chemical shifts that is in favor of a pyranose form concerned the *ca.* 20 ppm upfield shift of C-4′ signal with respect to those of dAdo (**9**). As a result, C-4′ resonates in the close proximity of C-3′. This may be explained by the fact that both C-3′ and C-4′ carbon atoms carry a hydroxyl group and have a CH_2 group in the α position. We also observe a *ca.* 10 ppm upfield of the C-1′ while the chemical shifts of the other carbon atoms are almost unchanged by comparison with those of dAdo (**9**).

The ^{15}N NMR spectroscopy provided clear and unambiguous information about such structures. Modern NMR methods allowed us to overcome the sensitivity problems associated with direct ^{15}N detection (low gyromagnetic ratio: −0.101 relative to protons and low natural abundance: 0.37%). This was achieved by using two-dimensional $^1H-^{15}N$ correlation experiments in which the proton magnetization is detected (*22*). Furthermore, complete ^{15}N resonance assignments were easily made possible by considering their scalar correlations with protons. The ^{15}N chemical shifts obtained for FAPyAde (**2**) and α-p-FAPydAdo (**5**) are shown in Table 3. Due to the difficulty in separating **2** and β-p-FAPydAdo (**3**) by RP-HPLC, the two-dimensional NMR experiments were not attempted on **3**. The ^{15}N signals at −299.1 ppm (FAPyAde (**2**)) and −297.9 ppm (α-p-FAPydAdo (**5**)) corresponding to the one-bond NH_2 protons scalar correlation were readily assigned to the exocyclic amine group at C-6 (and C-4 in the case of **2** for symmetrical reason). For the same reasons, the resonances at −259.1 and −260.8 ppm were assigned to the nitrogen atom of the formamido group of **2** and **5**, respectively. This is in agreement with the chemical shifts of *N*-substituted amides (*23*). However, the FAPy nucleoside **5** exhibits another NH-type nitrogen atom at −277.6 ppm attributed to N-4 on the basis of its $^1H-^{15}N$ scalar correlation. The noticeable downfield shift of N-4 observed in **5** with respect to **2** is probably due to the presence of the deoxyribose substituent, inducing an electronegative effect. N-1 and N-3 were attributed by their long-range correlation with H-2. The N-1 and N-3 of FAPyAde (**2**) appear as a single signal at −143.5 ppm. This may be explained by the equivalence of the two nitrogen atoms as the result of a symmetry within the molecule. In the case of α-p-FAPydAdo (**5**), N-1 (δ = −141.5 ppm) and N-3 (δ = −147.9 ppm) were distinguished from each other by their three-bond correlation with the NH_2-6 and NH-4 protons, respectively (Figure 2). This method appeared to be a relevant alternative to the use of specifically labeled compounds (*24*) for the assignment of purine nitrogen atoms.

Table 3. ^{15}N NMR Chemical Shifts[a] of the FAPy Derivatives (Major Rotamer)

δ (ppm)	N-1	N-3	N-5	N-4	N-6
FAPyAde (**2**)	−143.5	−143.5	−259.1	−299.1	−299.1[b]
α-p-FAPydAdo (**5**)	−141.5	−147.9	−260.8	−277.6	−297.9

[a] In ppm on the CH_3NO_2 scale. [b] Due to the symmetry of the molecule, the two NH_2 groups are equivalent.

Therefore, taking account all the above chemical and spectrometric data, a reasonable structure for the modified base of **3** and **5** is a FAPy derivative (Chart 1). ^1H and ^{13}C NMR features obtained in DMSO-d_6 clearly indicated the presence of a 2-deoxyribose moiety in both FAPy derivatives **3** and **5**. It should be added that the sugar moiety of both modified nucleosides exhibits a pyranose configuration. Confirmation was obtained by ^1H spin-coupling analysis of the 600.13 MHz ^1H NMR spectra in D_2O.

Characterization of the β Furanose FAPy Derivative (4). The mechanism of the formation of **3** and **5** may be rationalized in terms of initial addition of a hydroxyl radical •OH at the C-8 position of the base moiety of dAdo (**9**). The resulting radical undergoes a unimolecular ring-opening reaction at the C-8−N-9 bond in the absence of either oxygen or other oxidizing species (*14*). The last step is the reduction of the ring-opened radical, leading to the formation of the FAPy derivative. Consequently, all these reactions occurring within the microsecond time scale, the initial FAPy derivative must be produced in

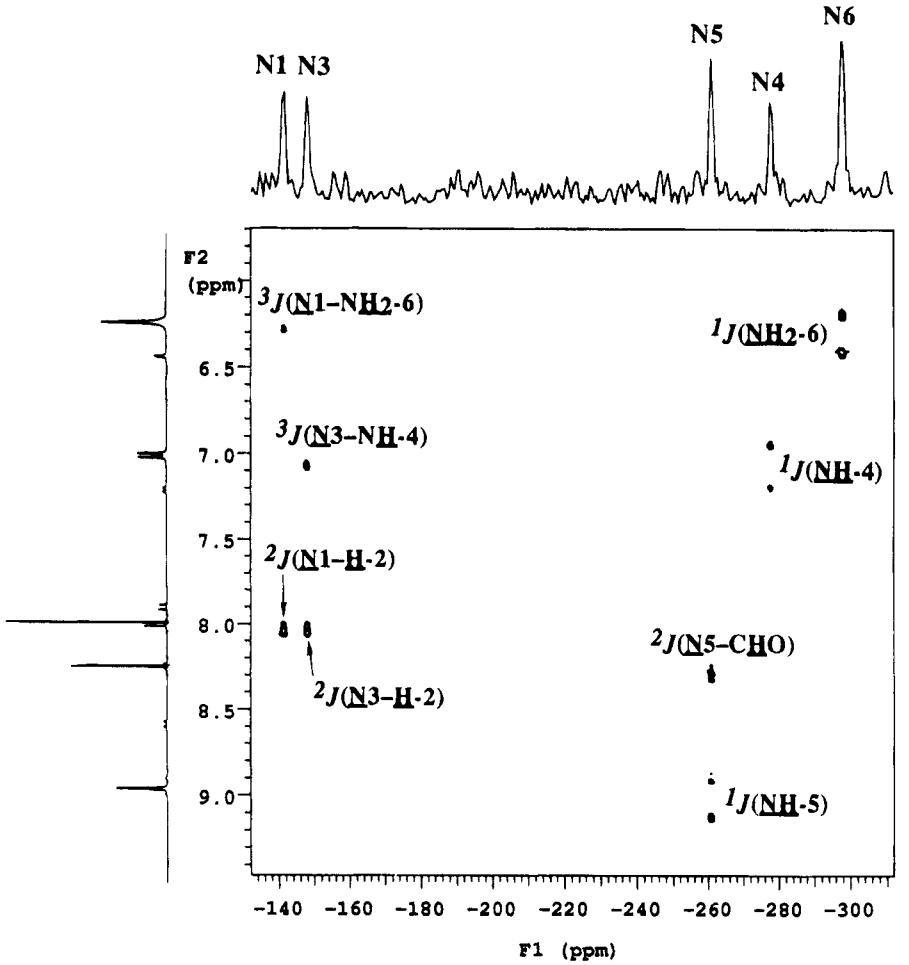

Figure 2. Long-range $^1H-^{15}N$ scalar-correlated 2D NMR spectrum (recorded with the HMBC sequence) of α-p-FAPydAdo (**5**). F1 and F2 are the ^{15}N and ^1H dimensions, respectively. ^1J(N-H) are residual intense correlations.

the β furanose form **4**. However, only the pyranose isomers **3** and **5** have been isolated *(vide supra)*. This may be explained if one considers that isomerization takes place rapidly during the isolation of the radiation-induced decomposition products. In order to confirm this hypothesis, attempts were made to search for the presence of **4** in the γ-irradiated aqueous solution of dAdo (**9**) by using ^1H NMR spectroscopy as the analytical tool, as illustrated in Figure 3. A γ-irradiated deaerated aqueous solution of dAdo (**9**) was immediately concentrated, freeze-dried, and redissolved in D_2O prior to ^1H NMR analysis. The region of the resonance signal of the anomeric protons shows only three main patterns (spectrum A): the pseudo-doublet at 6.54 ppm and the large pseudo-triplet at 6.38 ppm were attributed to the (5′*R*)-8,5′-cyclo-2′-deoxyadenosine (**7**) and dAdo (**9**), respectively. Then, the pseudo-triplet resonating at 6.03 ppm is likely to correspond to the H-1′ signal of β-f-FAPydAdo (**4**). Confirmation was given by ^1H NMR analysis of the same irradiated sample, after leaving it for 7 h at room temperature (spectrum B): no changes (peak intensities and/or chemical shifts) were observed for the resonance signals at 6.54 and 6.38 ppm, but one can see the emergence of a doublet of doublet at 5.97 ppm with a concomitant decrease in the intensity of the anomeric proton of **4**. This pattern is characteristic of an α furanose sugar form (*25*) and hence was attributed to belong to **6**. In parallel, samples were injected onto the HPLC column in order to assign the fractions corresponding to the different isomers. The same observations were made: peak area of **7** and **9** remained unchanged,

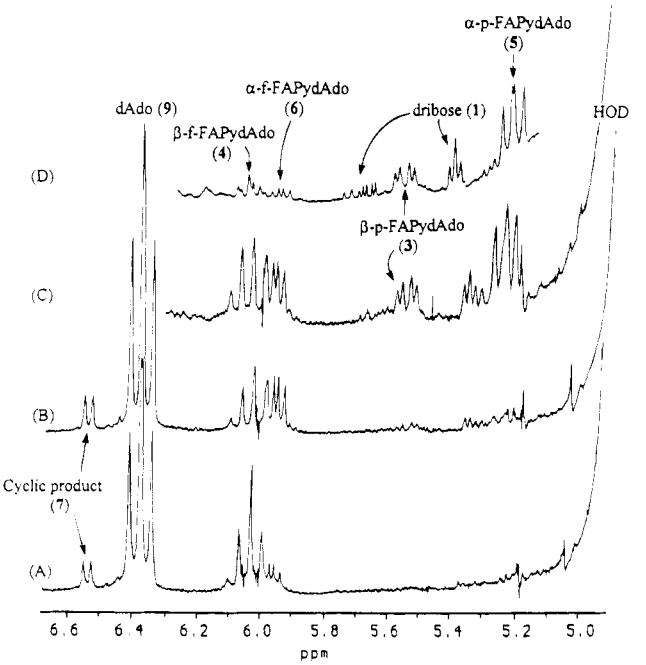

Figure 3. Part of the anomeric proton chemical shifts of the 200.13 MHz ^1H NMR spectrum in D_2O of γ-irradiated aqueous solution of dAdo in deaerated medium. (A) Immediately after irradiation. (B) After 7 h at 20 °C. (C) 26 h at 20 °C. (D) 72 h at 20 °C.

whereas a drastic reduction of the peak area of **4** with the enhancement of **6** occurred.

Chart 2

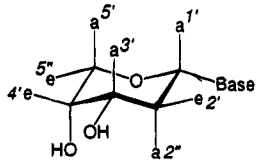

2-deoxy-α-D-ribopyranosyl FAPydAdo (**5**)

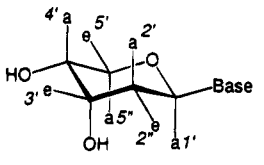

2-deoxy-β-D-ribopyranosyl FAPydAdo (**3**)

Table 4. 600.13 MHz ^{1}H NMR in D_2O

Coupling Constants (Hz)[a] of β-p-FAPydAdo (3) and α-p-FAPydAdo (5). Comparison with the Pyranose Forms of 2'-Deoxyadenosine[b]									
$J_{i\text{-}j}$ (Hz)	$J_{1'\text{-}2'}$	$J_{1'\text{-}2''}$	$J_{2'\text{-}2''}$	$J_{2'\text{-}3'}$	$J_{2''\text{-}3'}$	$J_{3'\text{-}4'}$	$J_{4'\text{-}5'}$	$J_{4'\text{-}5''}$	$J_{5'\text{-}5''}$
β-p-dAdo	10.3	2.3	−13.9	2.3	4.4	3.9	5.0	10.7	−11.5
α-p-dAdo	1.7	10.8	−12.1	4.6	11.7	2.7	1.7	1.3	−13.1
β-p-FAPydAdo (**3**)	9.8	2.6	−14.1	3.0	5.1	3.1	4.7	9.8	−11.4
α-p-FAPydAdo (**5**)	2.5	10.1	−12.6	4.6	11.1	3.2	3.1	1.4	−12.7
	Chemical Shifts (ppm) of β-p-FAPydAdo (3) and α-p-FAPydAdo (5)								
δ (ppm)	H-1'	H-2'	H-2"	H-3'	H-4'	H-5'	H-5"	H-2	CHO
β-p-FAPydAdo (**3**)	5.60	2.06	2.13	4.28	3.89	3.78	3.86	8.07	8.38
α-p-FAPydAdo (**5**)	5.34	2.05	2.01	4.09	3.91	3.94	3.78	8.06	8.48

[a] Estimated errors ± 0.1 Hz. [b] Taken from ref 17.

However, the two furanose anomers are not stable, and the only FAPy derivatives isolable by semipreparative RP-HPLC exhibit a pyranose structure: after an incubation period of 72 h (spectrum D), the furanose forms **4** and **6** disappeared at the benefit of the pyranose isomers **3** and **5** together with a release of 2-deoxy-D-*erythro*-pentose (**1**) and FAPyAde (**2**).

The mechanism of isomerization is likely to involve the opening of the C-1'−O-4' bond, giving rise to a Schiff base intermediate. Depending on how and which nucleophile will react with the acyclic sugar derivative, the final product distribution will be different: if the OH-4' group is the nucleophilic agent, the α-f-FAPydAdo (**6**) will be formed as the kinetic product of the reaction. If the OH-5' attacks the imine group (on both sides), the β-p-FAPydAdo (**3**) and α-p-FAPydAdo (**5**) will be generated as the thermodynamic products. The two latter nucleophilic additions preferentially occur, due to the intramolecular character of the processes. However, H_2O can also react in a competitive way with the Schiff base according to an intermolecular process. Subsequent hydrolysis of the C=N bond is expected to give rise to the release of 2-deoxy-D-*erythro*-pentose (**1**) and FAPyAde (**2**) in equal amounts. It should be noted that hydrolysis of the N-glycosidic bond and sugar rearrangements occur spontaneously at pH7. A similar isomerization process of the *N*7-alkyl FAPy guanine was already described (*26*), but the reaction was found to occur in dilute alkaline solution.

Configurational and Conformational Features of the Sugar Moiety of 3 and 5. The large coupling constants $^3J_{i,j} > 9.0$ Hz, where *i* and *j* refer to the vicinal protons numbered as shown in Chart 2, together with the very small scalar coupling $^3J_{i,j} < 3.0$ Hz for several osidic protons (Table 4), are unusual for 2-deoxy-D-*erythro*-pentofuranosyl nucleosides (*27*). The only available exceptions involve the anhydro (5'-8) purine nucleosides, the (5'-6) cyclopyrimidine nucleosides (*28*), and the *trans-syn* (+) diastereoisomer of cyclobutadithymidine (*29*). A pyranose configuration appears to be a better alternative for both nucleosides **3** and **5**.

The low values of the $J_{4'\text{-}5'}$ and $J_{4'\text{-}5''}$ coupling constants of **5** (equatorial−axial and diequatorial conformations, respectively) are indicative of an equatorial orientation for the H-4'. Hence, the H-3' adopts an axial orientation and is involved in two axial−equatorial coupling constants ($J_{3'\text{-}4'}$ and $J_{2'\text{-}3'}$) and one diaxial coupling constant $J_{2''\text{-}3'} = 11.1$ Hz. This is not possible in a boat conformation; therefore, a chair conformation is more likely. Moreover, the large diaxial scalar coupling $J_{1'\text{-}2''}$ indicates that H-1' is predominantly axially oriented, with the bulky aglycon assuming an expected equatorial orientation. Concerning the anomer **3**, the large coupling constant $J_{4'\text{-}5''}$ is explained by a preferential *trans*-axial position of the related protons. The equatorial H-3' shows three equatorial−axial coupling constants giving a clear indication for a chair conformation. In the case of a boat conformation, H-2' and H-3' should be eclipsed. Then, $J_{2'\text{-}3'}$ should be very large according to the Karplus equation (see also ref 27). In addition, a large diaxial $J_{1'\text{-}2''}$ should be observed (an axial orientation for the base should be excluded for steric hindrance reasons). Indeed, the large coupling constant between H-1' and H-2' protons provides support for a chair conformation with the base also lying in an equatorial conformation. Thus, the faster eluting compound **3** is a β anomer which assumes predominantly a $^4C_1$ conformation whereas the α anomer **5** adopts a preferential $^1C_4$ conformation. Further support for the assignment of both pyranose anomers was provided by the presence of long-range scalar coupling across the W-path: in the β anomer **3**, the fully saturated system $H_{3'}-C_{3'}-C_{4'}-C_{5'}-H_{5'}$ is confined to a planar zig-zag configuration, and an effective $^4J_{3'\text{-}5'}$ coupling of 0.7 Hz was observed. For a similar reason, the α anomer **5** exhibits a $^4J_{2'\text{-}4'} = 0.65$ Hz which was due to the planar zig-zag $H_{2'}-C_{2'}-C_{3'}-C_{4'}-H_{4'}$ arrangement. Figures 4 and 5 show the 600.13 MHz ^{1}H NMR experimental and computer-simulated spectra of both isomers. It should be noted that similar analyses were also conducted at 400.13 MHz (data not shown) in order to check for the correct assignments. One can also add that all these coupling constants are in agreement with those obtained for the α and β pyranose anomers of dAdo (*17*). The α-p-FAPydAdo (**5**) is more stable than β-p-FAPydAdo (**3**). The latter nucleoside was found to undergo partial conversion to the α anomer **5** with a concomitant release of the free base FAPyAde (**2**) and 2-deoxy-D-*erythro*-pentose (**1**).

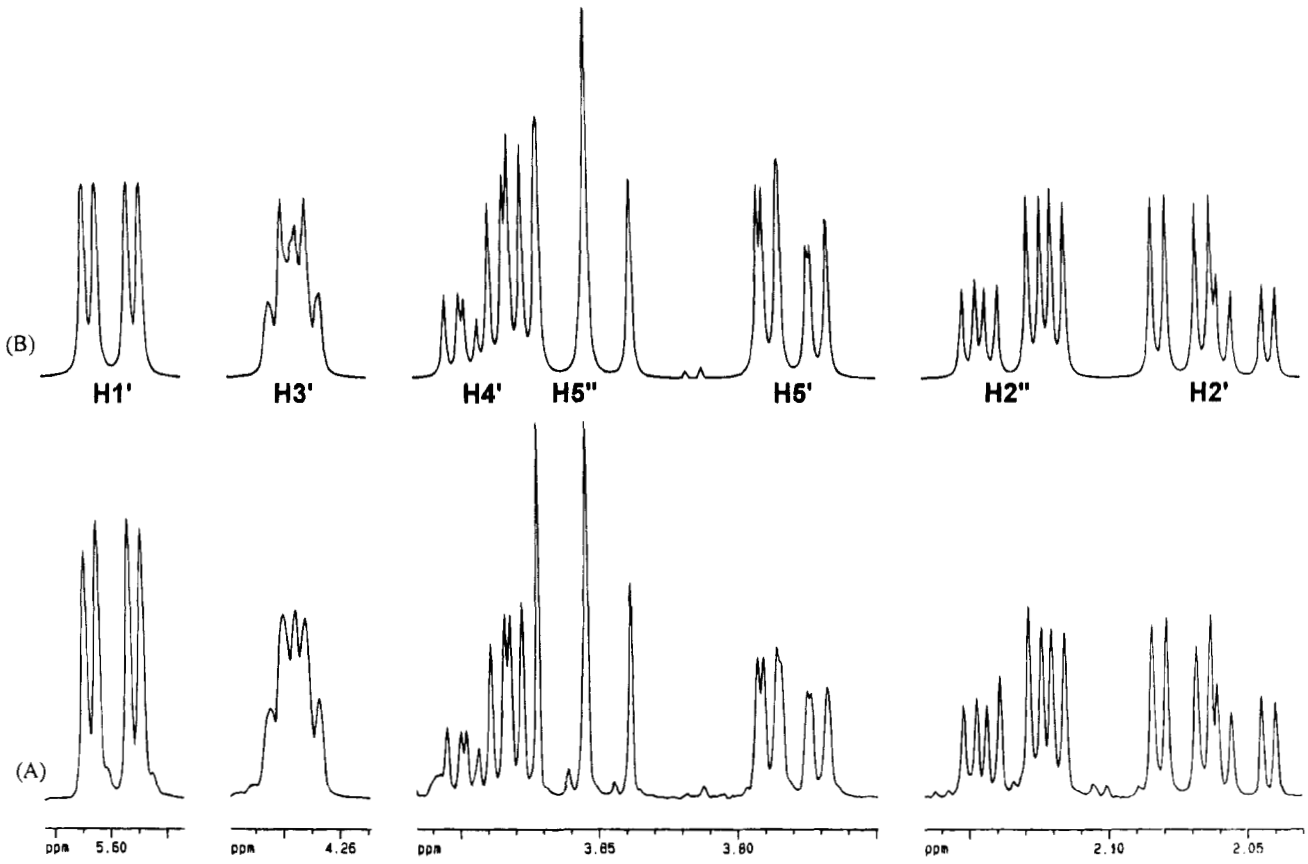

Figure 4. 600.13 MHz ^{1}H NMR spectra of 6-amino-4-[(2-deoxy-β-D-*erythro*-pentopyranosyl)amino]-5-(formylamino)pyrimidine (**3**) in D_2O. (A) Experimental spectrum. (B) Simulated spectrum.

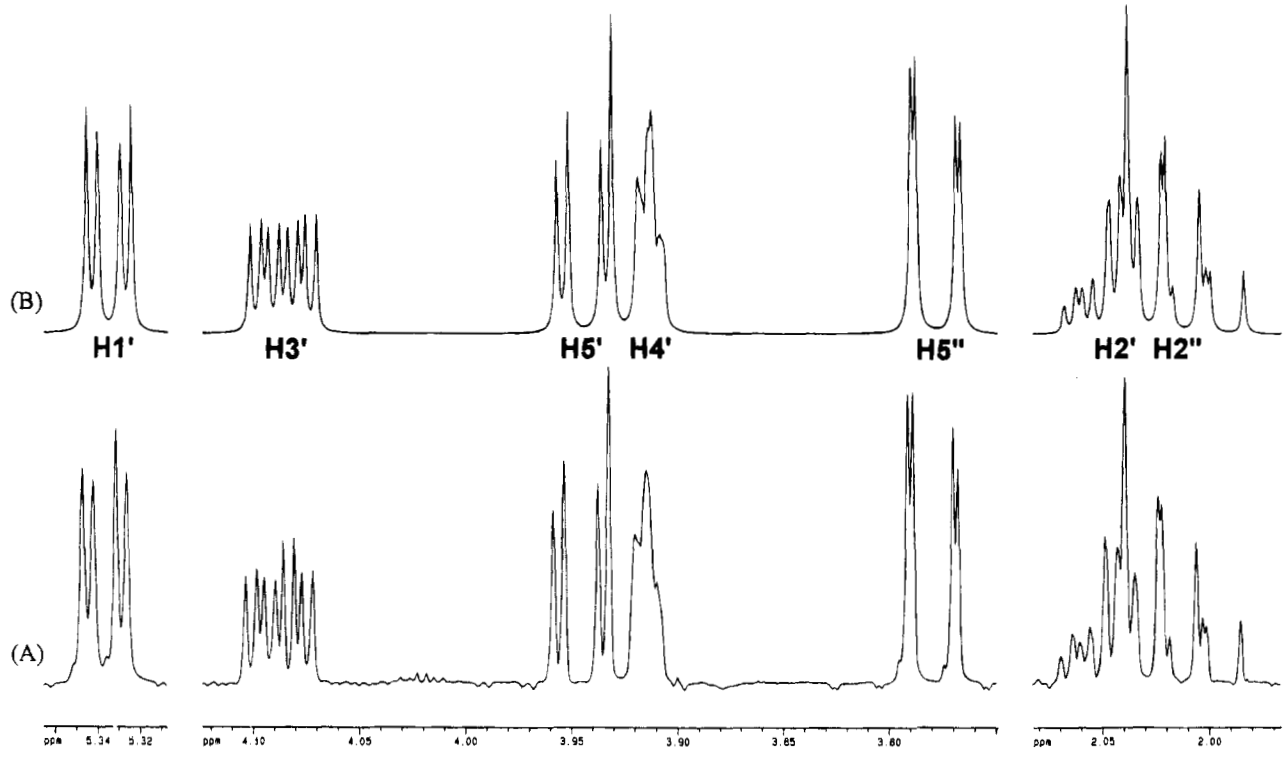

Figure 5. 600.13 MHz ^{1}H NMR spectra of 6-amino-4-[(2-deoxy-α-D-*erythro*-pentopyranosyl)amino]-5-(formylamino)pyrimidine (**5**) in D_2O. (A) Experimental spectrum. (B) Simulated spectrum.

^{1}H NMR Determination of the Rotational Barrier in the FAPy Derivatives. The presence of the formamido group in the FAPy derivatives **2**, **3**, and **5** raises the question of the restricted rotation of the amide bond due to the partial π character of the formylamine (N–CO) bond. This may lead to separate NMR spectra for the *s-cis* and *s-trans* isomers as already observed for a series of unsymmetrically N-substituted amides (*23*). Accordingly, the ^{1}H and ^{13}C NMR spectra of both FAPy derivatives show a minor set of signals. Chart 3 repre-

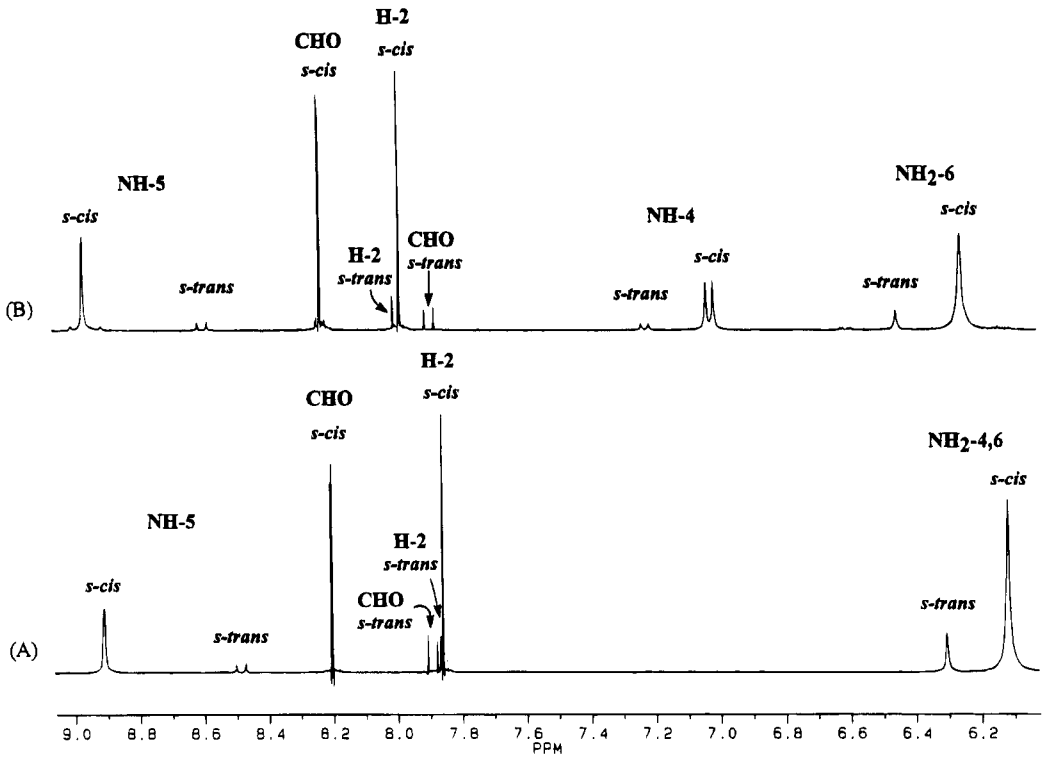

Figure 6. Low field region of the 400.13 MHz ^{1}H NMR spectra in DMSO-d_6 of (A) FAPyAde (**2**) and (B) α-p-FAPydAdo (**5**).

Chart 3

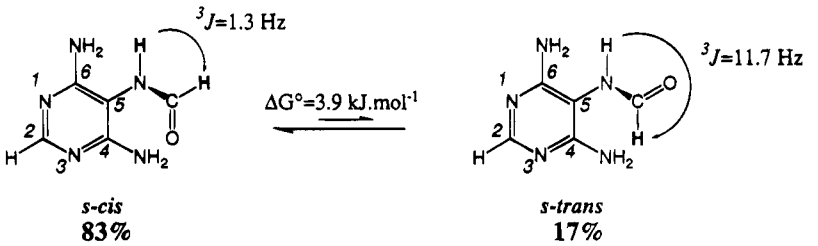

sents the two rotamers of FAPyAde (**2**) at 295 K in DMSO-d_6. The isomer percentage of FAPyAde (**2**) (major = 83%; minor = 17% at 295 K) was determined by integrating the well-separated NH_2-4,6 protons resonance in the high field region (major: 6.07 ppm; minor: 6.26 ppm) of ^{1}H NMR spectra obtained in DMSO-d_6. For the corresponding nucleosides **3** and **5**, the same ratio was observed; furthermore, the NH_2-6 and also the NH-4 signals are 0.2 ppm downfield shifted with respect to the corresponding signals of the major isomer. The chemical shifts of the anomeric protons H-1′ are much less affected ($\Delta\delta$ < 0.04 ppm) whereas those of the other protons of the sugar moiety and also the H-2 proton are not modified by the rotameric effect. The main difference concerns the NH-5 and CHO proton chemical shifts. The latter two protons of the minor rotamer of each of the FAPy derivatives **2**, **3**, and **5** resonate at higher field than the respective major rotamer: the NH-5 proton appears as a doublet (^3J(H,H) = 11.7 Hz) with a 0.4 ppm upfield shift. The CHO proton experiences a 0.3 ppm upfield shift and resonates as a doublet, with the same coupling constant (see Figure 6). The two-dimensional ^{1}H−^{1}H COSY analysis of the FAPyAde (**2**) confirmed the splitting of 11.7 Hz in the minor rotamer. This large coupling constant, associated with the small (^3J(H,H) = 1.3 Hz) value for the major rotamer,[2] is in line with the *trans* NH−CHO orientation of the so-called *s-trans* rotamer (minor) and a *cis* orientation of a *s-cis* rotamer (major). This result is consistent with the 12−88% relative importance (*s-trans*, *s-cis*, respectively) found for the two rotameric forms of the open imidazole ring of 7-methylguanine (*30*). It should be noted that similar observations were made in the ^{13}C NMR spectra of each of the FAPy derivatives: all the carbon signals of the base moiety of the minor rotamers experience a downfield shift with respect to the corresponding carbon resonances of the *s-cis* rotamer. The C=O signal (δ = 165.5 ppm) undergoes the most important shift ($\Delta\delta$ = 4.8 ppm); this large downfield shift is of the same order of magnitude as those observed in a series of unsymmetrically N-substituted amides (*23*): the carbonyl and the α-N carbon atoms always resonate at a higher field in the *s-cis* isomer with respect to the *s-trans* rotamer. Accordingly, the C-4 or C-6 signals of the *s-trans* rotamer are 1.2 ppm downfield shifted by comparison with those of the major *s-cis* rotamer whereas the C-2 and C-5 are less affected ($\Delta\delta$ = 0.4 ppm).

The barrier to amide bond rotation was then determined by measuring the change in ^{1}H NMR line shapes as a function of the temperature (*31*). The dynamic study was only conducted on the more stable FAPy derivative, *i.e.*, the FAPyAde (**2**), in order to avoid isomerization of

[2] The broadening of the NH-5 signal, which is due to the electric quadrupole moment of ^{14}N nucleus, hinders the observation of the small coupling constant.

the sugar moiety of **3** and **5** under heating. At first, the position of the equilibrium *s-cis*–*s-trans* (see Chart 3) was determined by the free energy of the process, $\Delta G°$, given by:

$$\Delta G° = -RT \ln([s\text{-}trans]/[s\text{-}cis]) \quad (1)$$

where R = gas constant and T = absolute temperature. At 295 K, when the exchange is slow, $\Delta G° = 3.9$ kJ·mol^{-1}. The rate of interconversion is determined by $\Delta G^{\#}$, the free energy of activation; this rate constant k is given by the Eyring equation:

$$k = (k_B/h)T \exp(-\Delta G^{\#}/RT) \quad (2)$$

where k_B = Boltzmann's constant and h = Planck's constant. At the coalescence, the following equation affords the rate constant k_c of the exchange at the coalescence temperature T_c, where $\Delta\nu$ is the chemical shift difference (Hz) for a given nucleus in the two rotamers when the exchange is slow:

$$k_c = (\pi/\sqrt{2})\Delta\nu \quad (3)$$

If this k_c is substituted into the Eyring equation (2), the free energy of activation from the coalescence point and temperature is obtained. By substituting numerical values of all constants, this equation may be written as follows:

$$\Delta G_c^{\#} \text{ (kJ·mol}^{-1}) = 8.314T_c\{22.96 + \ln(T_c/\Delta\nu)\} \quad (4)$$

To evaluate the free energy of activation associated with the conversion of the *s-cis* rotamer into the *s-trans* rotamer, the coalescence temperature was measured for the NH_2-4,6 protons in DMSO-d_6 (T_c = 370 K). Thus, with $\Delta\nu$ = 75.81 Hz measured at 295 K,

$$\Delta G_{370}^{\#} = (75.5 \pm 1.1) \text{ kJ·mol}^{-1}$$

This value is a little less than those reported for various *N*-alkyl amides (about 87.4 kJ·mol^{-1} (390 K) (*32*)). This may be explained by the steric hindrance of the bulky pyrimidine ring which is known to lower the energy barrier. Nevertheless, the calculated value is much more consistent with the 76.5 kJ·mol^{-1} (369 K) found for *N*-(2-deoxy-β-D-*erythro*-pentofuranosyl)formamide (*33*). However, solvent effects are known to modify the energy barrier, and thus comparison of various data reported in the literature is critical. Moreover, the present investigation confirms the rotameric nature of the observed isomerism. This rules out the involvement of a regioisomerism, in agreement with similar conclusions already made for *N*7-alkyl FAPy guanosine derivatives (*34*).

Conclusion

The opening of the imidazole ring constitutes the main radiation-induced degradation pathway of dAdo (**9**) in deaerated aqueous solutions. The isolation and characterization of FAPy derivatives of adenine should facilitate their search in •OH-mediated decomposition of DNA. However, the exact distribution of the α and β furanose anomers and the *s-cis* and *s-trans* rotamers within DNA remains to be determined. In addition, attempts are currently made to further establish whether FAPyAde is a substrate (*35*) or not (*36*) for formamidopyrimidine–DNA glycosylase (the Fpg protein), a well-characterized *Escherichia coli* DNA repair enzyme.

Acknowledgment. We thank Marie-Françoise Foray (Institut de Biologie Structurale, Grenoble) for recording the 600.13 MHz NMR spectra.

References

(1) Goodhead, D. T., Thacker, J., and Cox, R. (1993) Effects of radiation of different qualities on cells: molecular mechanism of damage and repair. *Int. J. Radiat. Biol.* **63**, 536–543.
(2) Ward, J. F. (1988) DNA damage produced by ionizing radiation in mammalian cells. Identities, mechanism of formation and repairability. *Prog. Nucleic Acid Res. Mol. Biol.* **35**, 95–125.
(3) von Sonntag, C. (1987) *The chemical basis of radiation biology*, Taylor and Francis, London.
(4) Bertinchamps, A. J., Hüttermann, J., Köhnlein, W., and Téoule, R. (1978) *Effects of ionizing radiation on DNA*, Springer, Berlin.
(5) Cadet, J. (1994) DNA damage caused by oxidation, deamination, ultraviolet radiation and photoexcited psoralens. In *DNA Adducts: Identification and Biological Significance* (Hemminki, K., Dipple, A., Shuker, D. E. G., Kadlubar, F. F., Segerbäck, D., and Bartsch, H., Eds.) IARC Scientific Publications 125, pp 245–276, International Agency for Research on Cancer, Lyon.
(6) Wagner, J. R., van Lier, J. E., Berger, M., and Cadet, J. (1994) Thymidine hydroperoxides. Structural assignment, conformational features, and thermal decomposition in water. *J. Am. Chem. Soc.* **116**, 2235–2242.
(7) Wagner, J. R., van Lier, J. E., Decarroz, C., Berger, M., and Cadet, J. (1990) Photodynamic methods for oxy radical-induced DNA damage. *Methods Enzymol.* **186**, 502–511.
(8) Téoule, R. and Cadet, J. (1978) Radiation-induced degradation of the base component in DNA and related substances—Final products. *Mol. Biol. Biochem. Biophys.* **27**, 171–203.
(9) Becker, P., and Sevilla, M. D. (1993) The chemical consequences of radiation damage to DNA. *Adv. Radiat. Biol.* **17**, 121–180.
(10) Steenken, S. (1989) Purine bases, nucleosides, and nucleotides: aqueous solution redox chemistry and transformation reactions of their radical cations and e^- and OH adducts. *Chem. Rev.* **89**, 503–520.
(11) Cadet, J., and Berger, M. (1985) Radiation-induced decomposition of the purine bases within DNA and related compounds. *Int. J. Radiat. Biol.* **47**, 127–143.
(12) Vieira, A. J. S. C., and Steenken, S. (1987) Pattern of OH radical reaction with 6- and 9-substituted purines. Effect of substituents on the rates and activation parameters of the unimolecular transformation reactions of two isomeric OH adducts. *J. Phys. Chem.* **91**, 4138–4144.
(13) Kasai, H., and Nishimura, S. (1991) Formation of 8-hydroxydeoxyguanosine in DNA by oxygen radicals and its biological significance. In *Oxidative Stress, Oxidants and Antioxidants* (Sies, H., Ed.) pp 99–116, Academic Press, New York.
(14) Vieira, A. J. S. C., and Steenken, S. (1990) Pattern of OH radical reaction with adenine and its nucleosides and nucleotides. Characterization of two types of isomeric OH adduct and their unimolecular transformation reactions. *J. Am. Chem. Soc.* **112**, 6986–6994.
(15) Berger, M., and Cadet, J. (1985) Isolation and characterization of the radiation-induced degradation products of 2′-deoxyguanosine in oxygen-free aqueous solutions. *Z. Naturforsch.* **40b**, 1519–1531.
(16) van Hemmen, J. J., and Bleichrodt, J. F. (1971) The decomposition of adenine by ionizing radiation. *Radiat. Res.* **46**, 444–456.
(17) Mariaggi, N., Téoule, R., Cadet, J., Dickie, H., and Hughes, E. (1979) A new radiolysis mechanism for 2′-deoxyadenosine in aqueous deaerated solution. *Radiat. Res.* **79**, 431–438.
(18) Mariaggi, N., Cadet, J., and Téoule, R. (1976) Cyclisation radicalaire de la désoxy-2′-adénosine en solution aqueuse, sous l'effet du rayonnement gamma (γ-Radiolytic induced radical cyclization of 2′-deoxyadenosine in aqueous solution). *Tetrahedron* **32**, 2385–2387.
(19) Martin, G. J., Martin, M. L., and Gouesnard, J.-P. (1981) ^{15}N-NMR Spectroscopy. *NMR Basic Principles and Progress*, Springler-Verlag, Berlin, Heidelberg, and New York.
(20) Kuo, K. C., McCune, R. A., and Gehrke, C. W. (1980) Quantitative reversed-phase high performance liquid chromatography determination of major and modified deoxyribonucleosides in DNA. *Nucleic Acids Res.* **8**, 4763–4776.
(21) Cho, B. P. (1993) Structure of oxidatively damaged nucleic acid adducts: pH dependence of the ^{13}C NMR spectra of 8-oxoguanosine and 8-oxoadenosine. *Magn. Reson. Chem.* **31**, 1048–1053.

(22) Bax, A., Giffey, R. H., and Hawkins, B. L. (1983) Sensitivity-enhanced correlation of ^{15}N and ^{1}H chemical shifts in natural-abundance samples via multiple quantum coherence. *J. Am. Chem. Soc.* **105**, 7188–7190.

(23) Dorie, J., Gouesnard, J. P., Mechin, B., Naulet, N., and Martin, G. J. (1980) Applications of ^{15}N NMR spectroscopy to the study of unsymmetrically *N*-substituted amides and model peptide compounds. *Org. Magn. Reson.* **13**, 126–131.

(24) Gonnella, N. C., Nakanishi, H., Holtwick, J. B., Horowitz, D. S., Kanamori, K., Leonard, N. J., and Roberts, J. D. (1983) Studies of tautomers and protonation of adenine and its derivatives by nitrogen-15 nuclear magnetic resonance spectroscopy. *J. Am. Chem. Soc.* **105**, 2050–2055.

(25) Cadet, J., Taïeb, C., Remin, M., Niemczura, W. P., and Hruska, F. E. (1980) Conformational studies of α- and β-pyrimidine 2′-deoxyribonucleosides in the *syn* and *anti* conformation. *Biochim. Biophys. Acta* **608**, 435–445.

(26) Tomasz, M., Lipman, R., Lee, M. S., Verdine, G. L., and Nakanishi, K. (1987) Reaction of acid-activated mitomycin C with calf thymus DNA and model guanines: elucidation of the base-catalyzed degradation of *N7*-alkylguanine nucleosides. *Biochemistry* **26**, 2010–2027.

(27) Altona, C., and Sundaralingam, M. (1973) Conformational analysis of the sugar ring in nucleosides and nucleotides. Improved method for the interpretation of proton magnetic resonance coupling constants. *J. Am. Chem. Soc.* **95**, 2333–2344.

(28) Shaw, A. A., and Cadet, J. (1988) Formation of cyclopyrimidines via the direct effects of gamma radiation of pyrimidine nucleosides. *Int. J. Radiat. Biol.* **54**, 987–997.

(29) Cadet, J., Voituriez, L., Hruska, F. E., Kan, L.-S., de Leeuw, F. A. A. M., and Altona, C. (1985) Characterization of thymidine ultraviolet photoproducts. Cyclobutane dimers and 5,6-dihydrothymidines. *Can. J. Chem.* **63**, 2861–2868.

(30) Boiteux, S., Belleney, J., Roques, B. P., and Laval, J. (1984) Two rotameric forms of open ring 7-methylguanine are present in alkylated polynucleotides. *Nucleic Acids Res.* **12**, 5429–5439.

(31) Kessler, H. (1970) Detection of hindered rotation and inversion by NMR spectroscopy. *Angew. Chem., Int. Ed. Engl.* **9**, 219–235.

(32) Oki, M. (1985) Applications of dynamic NMR spectroscopy to organic chemistry. *Methods Stereochem. Anal.* **4**, VCH Publishers, Deerfield Beach, FL.

(33) Cadet, J., Nardin, R., Voituriez, L., Remin, M., and Hruska, F. E. (1981) A ^{1}H and ^{13}C NMR study of the radiation-induced degradation products of 2′-deoxythymidine derivatives: N-(2-deoxy-β-D-*erythro*-pentofuranosyl)formamide. *Can. J. Chem.* **59**, 3313–3318.

(34) Humphreys, W. G., and Guengerich, F. P. (1991) Structure of formamidopyrimidine adducts as determined by NMR using specifically ^{15}N-labeled guanosine. *Chem. Res. Toxicol.* **4**, 632–636.

(35) Boiteux, S., Gajewski, E., Laval, J., and Dizdaroglu, M. (1992) Substrate specificity of the *Escherichia coli* Fpg protein (formamidopyrimidine–DNA glycosylase): excision of purine lesions in DNA produced by ionizing radiation or photosensitization. *Biochemistry* **31**, 106–110.

(36) Tchou, J., Bodepudi, V., Shibutani, S., Antoshechkin, I., Miller, J., Grollman, A. P., and Johnson, F. (1994) Substrate specificity of Fpg protein. *J. Biol. Chem.* **269**, 15318–15324.

TX9500282